Multiscale Methods for Flow in Porous Media

Knut–Andreas Lie[*]**, Jørg E. Aarnes, Vegard Kippe, and Stein Krogstad**
Department Applied Mathematics
SINTEF ICT, Oslo, Norway
e–mail: Knut-Andreas.Lie@sintef.no

Summary We present a hierarchical multiscale method for the numerical solution of two-phase flow in strongly heterogeneous porous media. The method is based upon a mixed finite-element formulation, where basis functions are computed numerically on a coarse grid to correctly and accurately account for subscale permeability variations from an underlying (fine-scale) geomodel.

Introduction

Natural porous rock formations are heterogeneous at all length scales. When modelling fluid flow in porous formations, it is generally not possible to account for all pertinent scales, from the micrometre scale of pore channels to the kilometre scale of the full reservoir. Instead, one has to create models for studying phenomena occurring at a reduced span of length scale, and any modelling attempt should therefore generally be accompanied by appropriate rescaling (up- and downscaling) techniques.

Here we focus on how to incorporate fine-scale features from a detailed geomodel into flow simulations on a reservoir scale. Whereas industry-standard geomodels may contain between 10^6–10^9 grid cells, commercial reservoir simulators are typically capable of simulating models with 10^4–10^6 degrees of freedom. A large activity is therefore devoted to upscaling/downscaling between a detailed reservoir model and a coarser simulation model.

We present an alternative approach based on a multiscale formulation for pressure and flow velocities, where the global flow is computed on a coarse grid and fine-scale heterogeneity is accounted for through a set of generalised, heterogeneous basis functions. The basis functions are computed numerically by solving local flow problems (as is done in many flow-based upscaling methods), and when included in the coarse-grid equations, the basis functions ensure that the global equations are consistent with the local properties of the underlying differential operators. Several different multiscale methods have been proposed, including the multiscale mixed finite-element method (MsMFEM) [2], the multiscale finite-volume method [9], and numerical subgrid upscaling [6]. Common for all three methods is that they produce mass-conservative solutions both on the coarse grid and on the underlying fine grid, and they may thus be used either as very robust upscaling methods or as efficient fine-scale solvers.

Multiscale Mixed Finite Elements

The Two-Phase Flow Model
We consider incompressible flow of two phases (water and oil). For simplicity, we neglect the effects of gravity and capillary forces. The flow equations can then be formulated as an elliptic equation for the pressure p and total velocity v,

$$v = -(\lambda_w + \lambda_o)K\nabla p, \qquad \nabla \cdot v = q. \tag{1}$$

Here q is a source term representing injection and production wells, K is the rock permeability (i.e., the ability to transmit fluids), and $\lambda_\alpha = k_\alpha^r/\mu_\alpha$ is the mobility of phase α, where μ_α is viscosity of phase α and $k_\alpha^r = k_\alpha^r(S)$ is the relative permeability, i.e., the reduced ability of the rock to transmit fluids due to the presence of other phases. The saturation S denotes the volume fraction of water and is described by the transport equation

$$\phi\partial_t S + v \cdot \nabla f(S) = q_s, \tag{2}$$

where ϕ is the rock porosity and $f = \lambda_w/(\lambda_o + \lambda_w)$ is the fractional flow function.
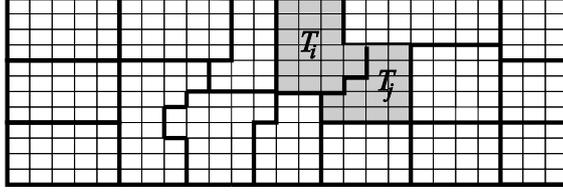
Figure 1: A general coarse grid overlying a uniform fine grid with the grey area giving the support of basis function ψ_{ij}.

Mixed Finite Elements

The mixed finite-element discretisation of the pressure equation (1) in a domain Ω seeks a pair $(v, p) \in U \times V$, where U and V are finite-dimensional subspaces of $H_0^{\mathrm{div}}(\Omega)$ and $L^2(\Omega)$, respectively, such that

$$\int_\Omega v \cdot (\lambda K)^{-1} u \; dx - \int_\Omega p \nabla \cdot u \; dx = 0, \qquad \text{for all } u \in U, \qquad (3)$$

$$\int_\Omega l \nabla \cdot v \; dx = \int q l \; dx, \qquad \text{for all } l \in V. \qquad (4)$$

Thus letting $\{\psi_i\}$ and $\{\phi_k\}$ be bases for $U \subset H_0^{\mathrm{div}}(\Omega)$ and $V \subset L^2(\Omega)$, we obtain approximations $v = \sum v_i \psi_i$ and $p = \sum p_k \phi_k$, where the coefficients $\mathbf{v} = \{v_i\}$ and $\mathbf{p} = \{p_k\}$ solve a linear system of the form

$$\begin{bmatrix} \mathbf{B} & \mathbf{C} \\ \mathbf{C}^T & \mathbf{O} \end{bmatrix} \begin{bmatrix} \mathbf{v} \\ -\mathbf{p} \end{bmatrix} = \begin{bmatrix} \mathbf{0} \\ \mathbf{q} \end{bmatrix}, \qquad (5)$$

where

$$b_{ij} = \int_\Omega \psi_i \cdot (\lambda K)^{-1} \psi_j \; dx, \quad c_{ik} = \int_\Omega \phi_k \nabla \cdot \psi_i \; dx, \quad \text{and} \quad q_k = \int_\Omega \phi_k q \; dx.$$

Multiscale Basis Functions

In a standard discretisation, the spaces U and V typically consist of low-order piecewise polynomials. In the multiscale methods, U and V are given by the solution of local flow problems. Let $\mathcal{K} = \{K_m\}$ be a partitioning of Ω into mutually disjoint grid cells. Furthermore, let $\mathcal{T} = \{T_i\}$ be a coarser partitioning of Ω, in such a way that whenever $K_m \cap T_i \neq 0$ then $K_m \subset T_i$; see Figure 1. Let Γ_{ij} denote the non-degenerate interfaces $\Gamma_{ij} = \partial T_i \cap \partial T_j$. For each Γ_{ij} we assign a basis function $\psi_{ij} \in U_{\mathrm{ms}}$, and for each T_i we assign a basis function $\phi_i \in V$. The basis function ψ_{ij} is obtained by forcing a unit flow from cell T_i to T_j; that is, by solving a local flow problem in $\Omega_{ij} = T_i \cup T_j$

$$\psi_{ij} = -\lambda K \nabla \phi_{ij}, \quad \nabla \cdot \psi_{ij} = \begin{cases} w_i(x), & \text{for } x \in T_i, \\ -w_j(x), & \text{for } x \in T_j, \end{cases} \qquad (6)$$

with $\psi \cdot \nu = 0$ on $\partial \Omega_{ij}$, where ν is the outward-pointing unit normal to $\partial \Omega_{ij}$. To give a unit flow from T_i to T_j, the source terms $w_i(x)$ are normalized

$$w_i(x) = W_i(x) \cdot \left(\int_{T_i} W_i(\xi) \; d\xi \right)^{-1}. \qquad (7)$$

Here $W_i = q$ for cells containing a well (i.e., for all T_i for which $\int_{T_i} q \neq 0$). This choice ensures a conservative approximation of v on the fine grid. For all other cells, we choose $W_i(x) = 1$ or $W_i(x) = \mathrm{trace}(K(x))$. The corresponding basis functions can be seen as generalisations of the lowest-order Raviart–Thomas basis functions in a standard mixed method. Figure 2 illustrates the x-velocity basis functions in two different cases.
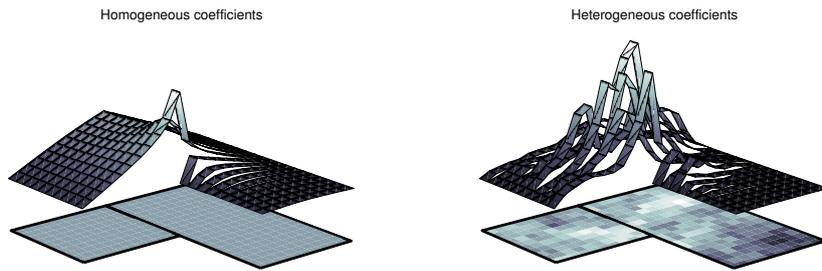
Figure 2: The x component of the velocity basis function associated with an edge between two cells of different size for a homogeneous and a heterogeneous permeability field, respectively.
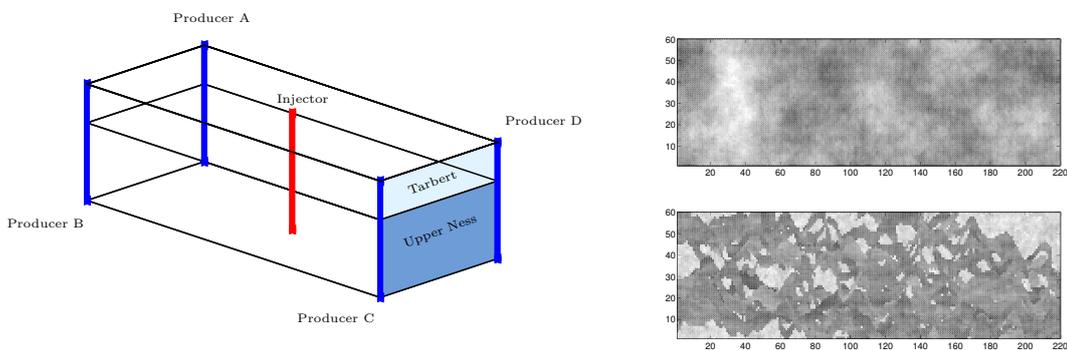

Figure 3: Schematic of the SPE10 reservoir model. The reservoir dimensions are $1200 \times 2200 \times 170$ ft., and the model consists of $60 \times 220 \times 85$ grid cells. The top and bottom plots to the right depict the logarithm of the horizontal permeability in the top layer of the Tarbert formation and the bottom layer of the Upper Ness formation.

Discussion

In this section we show that MsMFEM: (i) is an accurate and robust alternative to upscaling; (ii) is efficient when used as an approximate fine-scale solver for dynamic flow cases; and (iii) is very flexible with respect to the choice of coarse grid cells, given an appropriate fine-grid solver.

Accuracy and Robustness — 10th SPE Comparative Solution Project

Model 2 from SPE10 [7] was designed as a benchmark for various upscaling techniques and consists of two different rock formations; see Figure 3. Both formations are highly heterogeneous, with permeability variations of more than eight orders of magnitude, but are qualitatively different. The shallow-marine Tarbert formation is smooth, and therefore not too hard to upscale. The fluvial Upper Ness formation contains intertwined networks of high-permeability channels and poses severe challenges to any numerical method.

In Figure 4 we compare production curves from a MsMFEM simulation with a reference solution obtained by direct simulation on the full model. For the MsMFEM simulation we used a $5 \times 11 \times 17$ coarse grid and computed the fluid transport on the fine grid using fluxes from the corresponding subscale velocity field. For comparison, we also include results obtained from a upscaling/downscaling approach [8]. The MsMFEM is able to accurately reproduce the flow in the fine-scale channels and therefore matches the reference curves almost exactly. The upscaling/downscaling approach, on the other hand, does not properly account for the coupling between small-scale and large-scale effects and therefore fails to reproduce the production curves of the
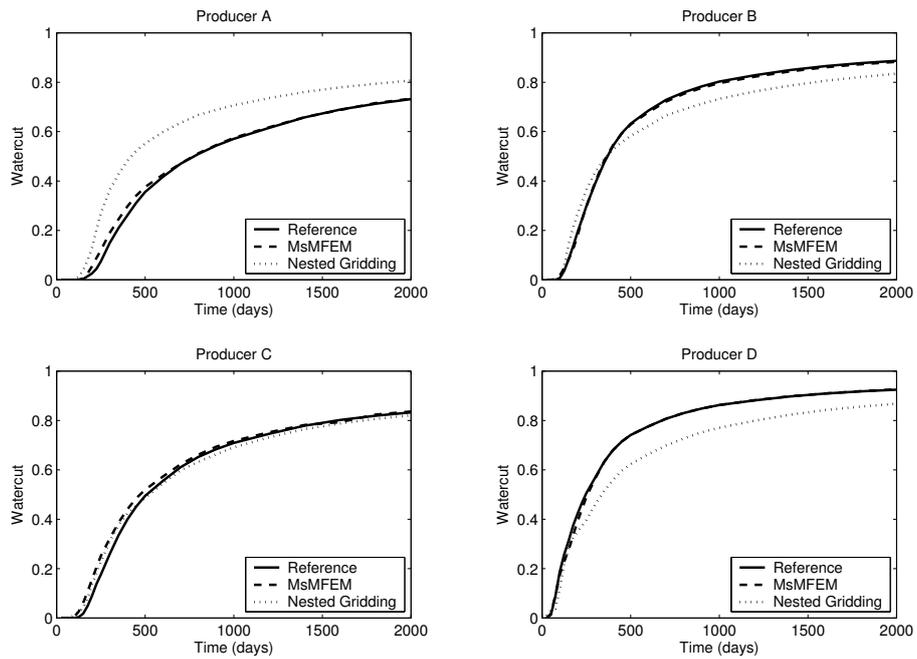
Figure 4: Water-cut curves after 2000 days of production for the SPE10 benchmark.
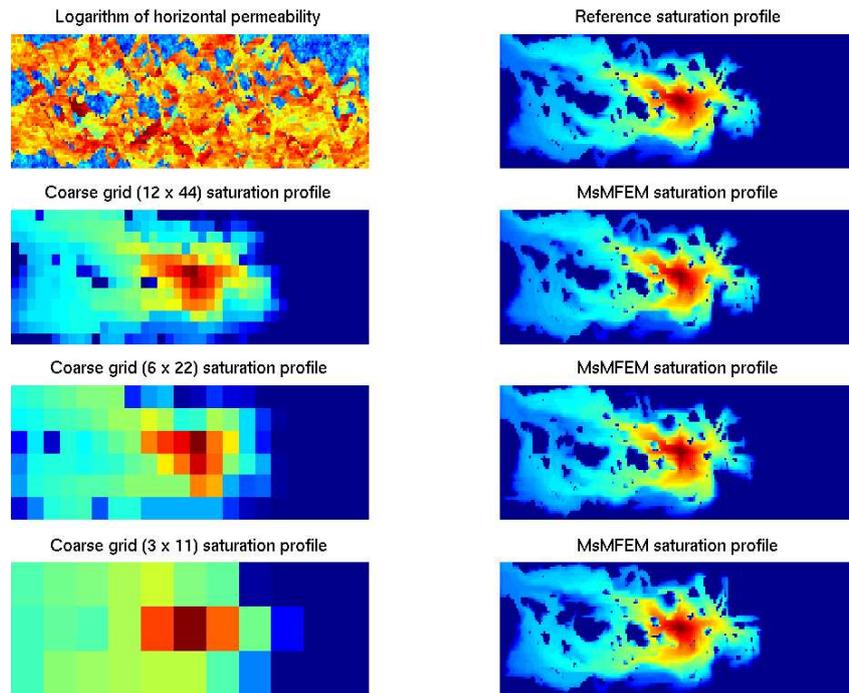

Figure 5: MsMFEM solutions for varying coarse grids on layer 85 from the SPE10 benchmark. In the left column, the coarse-grid fluxes are used to compute fluid transport, and in the right column, the subgrid fluxes are used to compute the transport on the original grid.
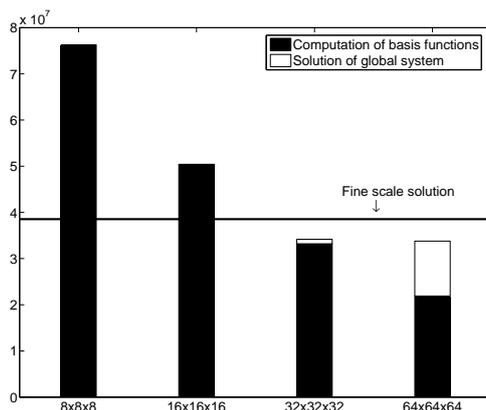
Figure 6: Computational work (idealised) for different coarse grids, assuming a Cartesian $128 \times 128 \times 128$ grid on the fine-scale.

individual wells correctly. See [3] for a more thorough discussion.

Next, we consider flow in the bottom layer computed using three different coarse grids with 12×44 cells, 6×22 cells, and 3×11 cells. Figure 5 compares saturation profiles obtained using the coarse-grid fluxes obtained by MsMFEM, and saturation profiles obtained on the fine 60×220 grid using the subgrid fluxes. The figure shows that the resolution is improved remarkably by utilising the inherent subgrid resolution rather than using MsMFEM as an advanced upscaling method. Moreover, it is evident that MsMFEM is robust with respect to the size of the coarse grid.

Computational Efficiency

Depending on the nonlinearity of the system (1)–(2), the pressure p may need to be recomputed several times throughout a simulation. In fact, the number of pressure solves in a typical flow case of water injection into a oil reservoir is of the order $\mathcal{O}(10^2)$. The key to the computational efficiency of the MsMFEM is the following observation: before the water front has swept through a coarse block T_i, the coefficient $\lambda(S)K(x)$ in (6) is constant (since S is constant), and after the waterfront has left the grid block, $\lambda(S)$ increases slowly. After the initial pressure solve, only a few basis functions ψ_{ij} close to the water front need to be recomputed [2], unless there is an abrupt change in the pressure field due to e.g., changing well configurations.

In Figure 6 we have plotted the computational cost for MsMFEM for different coarse grids compared with the cost of a direct solution on a uniform Cartesian grid with 128^3 grid blocks. The figure shows that the MsMFEM may not necessarily be more efficient than direct fine-scale solution for a single pressure solve, but it is also clear that the work associated with determining basis functions dominates the work associated with solving the global system. Hence, for a full simulation, where a minor fraction of the basis functions need to be updated in each pressure solve, the MsMFEM provides a potentially very large speedup. Moreover, since all basis function can be computed independent of each other, the MsMFEM has an inherent parallelism that can be exploited to speed up the computations.

Flexibility

A major advantage with the multiscale mixed formulation is the flexibility with respect to grids. A bit simplified this can be stated as follows: given an appropriate solver for the fine grid system, the multiscale method can be formulated and basis functions can be computed on (almost) any coarse grid where each grid block consists of an arbitrary collection of connected fine-grid cells. Moreover, numerical tests show that MsMFEM is *not very sensitive* to the shape of the coarse cells and accurate results are obtained for grids containing blocks with pretty 'exotic' shapes [5]. This means that the process of generating a coarse simulation grid from a complex
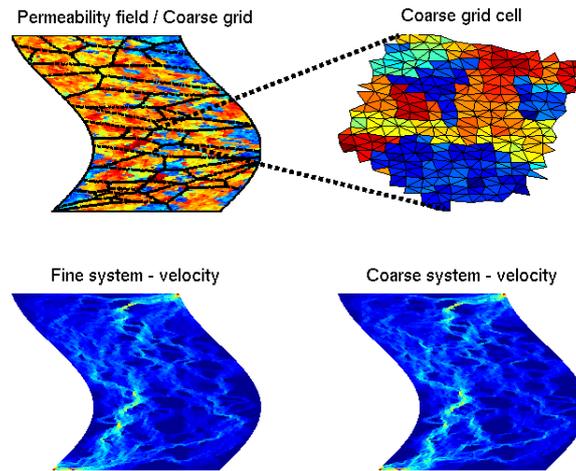
Figure 7: Comparison of flow velocity obtained direct simulation on an unstructured triangular grid and by MsMFEM on an unstructured coarse grid.
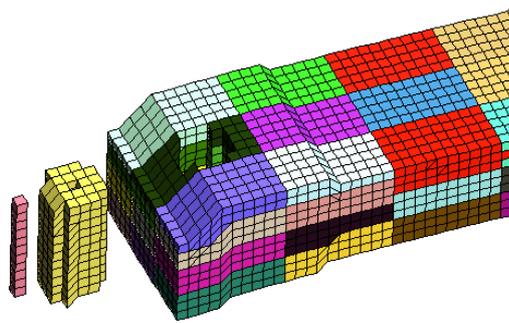

Figure 8: A coarse grid defined on top of a structured corner-point fine grid. The cells in the coarse grid are given by different colours.

geomodel can be greatly simplified, regardless of whether the fine grid is fully unstructured or is a structured corner-point grid with geometrical complications due to faults, throws, and eroded cells.

We end the paper by showing a few grid models to support the claim of the great flexibility inherent in MsMFEM. As the first example we consider an unstructured triangular fine grid in 2D. The coarse grid blocks in Figure 7 are formed as collections of fine-grid cells and can thus have almost arbitrary polygonal shape. The resulting grid contains cells that are (almost) triangular, quadrilateral, pentagonal, and hexagonal. By using unstructured triangular fine grids, it is easy to adapt both the fine grid and the coarse grid to complex external and internal boundaries.

As a next example, Figure 8 shows a vertical well penetrating a structured corner-point grid with eroded layers. On the coarse grid, the well is confined to a single cell consisting of all cells in the fine grid penetrated by the well. Moreover, notice the single neighbouring block shaped like a 'cylinder' with a hole.

Finally, Figure 9 shows a subsection of the SPE10 model, in which we have inserted a few flow barriers with very low permeability. In [5] it was shown that MsMFEM becomes inaccurate if coarse grid cells are cut into two (or more) non-communicating parts by a flow barrier. Fortunately, this can be automatically detected when generating basis functions, and the resolution can
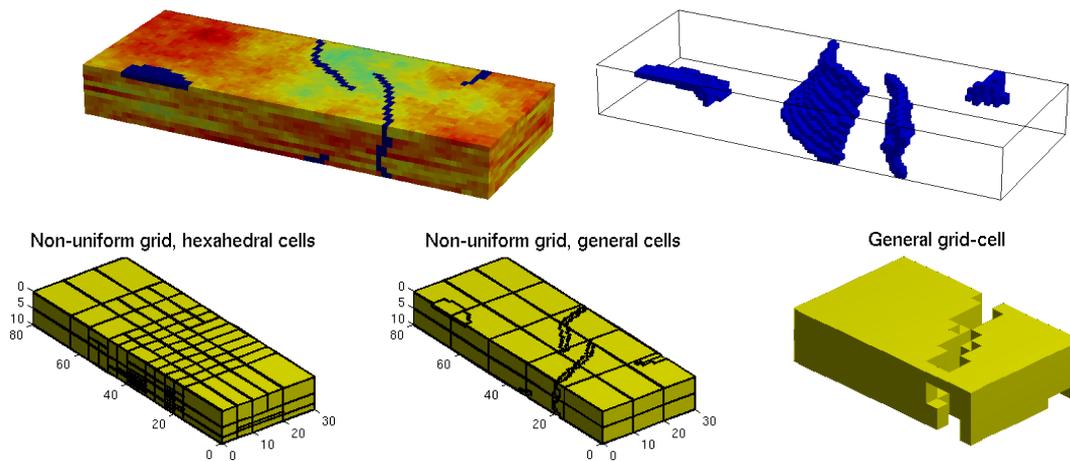
Figure 9: The upper row shows the permeability field (right), and the interior barriers (left). The lower row shows a hierarchically refined grid (left), the barrier grid (middle), and a coarse grid block in the barrier grid (right).

be improved by using some form of grid refinement. The figure shows two different approaches: (i) structured, hierarchical refinement, and (ii) direct incorporation of the flow barriers as extra coarse grid blocks intersecting a uniform $3 \times 5 \times 2$ grid. This results in rather exotic coarse cells, e.g., as shown in the figure, where the original rectangular cell consisting of $10 \times 16 \times 5$ fine cells is almost split in two by the barrier, and the resulting coarse cell is only connected through a single cell in the fine grid. Although the number of grid cells in the barrier grid is five times less than for the hierarchically refined grid, the errors in the production curves are comparable, indicating that MsMFEM is robust with respect to the shape of the coarse cells.

Concluding remarks

References

[1] Reservoir Simulation on a Geological Scale, http://www.math.sintef.no/GeoScale/.

[2] J. E. Aarnes. On the use of a mixed multiscale finite element method for greater flexibility and increased speed or improved accuracy in reservoir simulation. *Multiscale Model. Simul.*, **2(3)**, 421–439, (2004).

[3] J. E. Aarnes, V. Kippe, and K.-A. Lie. Mixed multiscale finite elements and streamline methods for reservoir simulation of large geomodels. *Adv. Water Resources*, **28(3)**, 257–271, (2005).

[4] J. E. Aarnes, V. Kippe, and K.-A. Lie. Multiscale methods and streamline simulation for rapid reservoir performance prediction. In A. Di Bucchianico, R. M. M. Mattheij, and M. A. Peletier, editors, *Progress in Industrial Mathematics at ECMI 2004*, Mathematics in Industry. Springer Verlag (2006).

[5] J. E. Aarnes, S. Krogstad, and K.-A. Lie A hierarchical multiscale method for two-phase flow based upon mixed finite elements and nonuniform coarse grids. *Multiscale Model. Simul.*, submitted.

[6] T. Arbogast. Numerical subgrid upscaling of two-phase flow in porous media. In Z. Chen et al, editors, *Numerical Treatment of Multiphase Flows in Porous Media*, Lecture Notes in Physics, vol. 552, pages 35–49, Springer Verlag, (2000).

[7] M. A. Christie and M. J. Blunt. Tenth SPE comparative solution project: A comparison of upscaling techniques. *SPE Res. Eng. Eval.*, **4**, 308–317, (2001), http://www.spe.org/csp/.

[8] Y. Gautier, M. J. Blunt, and M. A. Christie. Nested gridding and streamline-based simulation for fast reservoir performance prediction. *Comp. Geosci.*, **3**, 295–320, (1999).

[9] P. Jenny, S. H. Lee, and H. A. Tchelepi. Multi-scale finite-volume method for elliptic problems in subsurface flow simulation. *J. Comp. Phys.*, **187**, 47–67, (2003).